Comparison between Geostrophic Currents and Measured Currents in the Southwestern Part of the East Sea

CHANG-WOONG SHIN, SANG-KYUNG BYUN[1] AND CHEOLSOO KIM[1]

Department of Oceanography, Inha University, Inchon 402-751, Korea
[1]*Korea Ocean Research and Development Institute,*
Ansan P.O. Box 29. Seoul 425-600, Korea

A comparative study between geostrophic currents and directly measured currents was conducted for the upper layer to 200 m depth by using data from eleven observations of CTD and ADCP between March 1992 and November 1993 in the southwestern part of the East Sea. First-order linear relationship was found between calculated geostrophic currents and measured currents with the correlation coefficient of 0.83. On the average, 68.7% of directly measured current can be explained by geostrophic current obtained by dynamic method. The correlation coefficients increased with total geostrophic transport, which suggests that geostrophic balance is good in areas of strong current.

INTRODUCTION

Oceanic currents can be either directly measured or indirectly calculated from density structures. Recently, oceanic currents have often been measured by using satellite-tracked drifters or Acoustic Doppler Current Profilers (ADCP). ADCP measures multilayer currents either when ADCP is moored or when ADCP is mounted on the vessel.

There are various studies which explain the circulation with dynamic topography in the East Sea (Ohwada and Tanioka, 1972; Lee and Whang, 1981; etc.). Recently, other studies have attempted to compare current distribution between geostrophic currents and currents measured by ADCP (Kaneko *et al.*, 1991; Shin *et al.*, 1995; Lie *et al.*, 1995). However, these studies did not compare current speed quantitatively.

To determine layer of no motion is important because geostrophic current is relative speed to the reference layer. Some previous studies were carried out on the simple assumption that the current in deep layer is slow enough in the East Sea to take 700 m or 1000 m as layer of no motion (Ohwada and Tanioka, 1972; Shin *et al.*, 1995; Lie *et al.*,

1995). In the southern part of the East Sea, Lee (1978) chose 100 m as the reference layer because the overall depths in the Korea Strait, which the Tsushima Current passes through, are about 100 m. Others chose the layer of no motion with isopycnal or isothermal surface estimated from water-mass analysis in coastal areas, most of them were about 100 m depth (Seung, 1974; Byun and Seung, 1983; Lie and Byun, 1985).

In this study, the layer of no motion was chosen by minimum net transport method. Geostrophic currents calculated from CTD data in the southwestern part of the East Sea were compared with currents measured by ADCP. In addition, it was investigated as to what portion of the measured currents were the geostrophic currents.

DATA AND METHOD

For this study, the data gathered from eleven surveys at 70 stations in the southwestern part of the East Sea from March 1992 to November 1993 were used (Fig. 1). Water temperature and salinity were measured using the CTD system (Neil Brown Mark IIIB) from sea surface to sea bed and averaged at
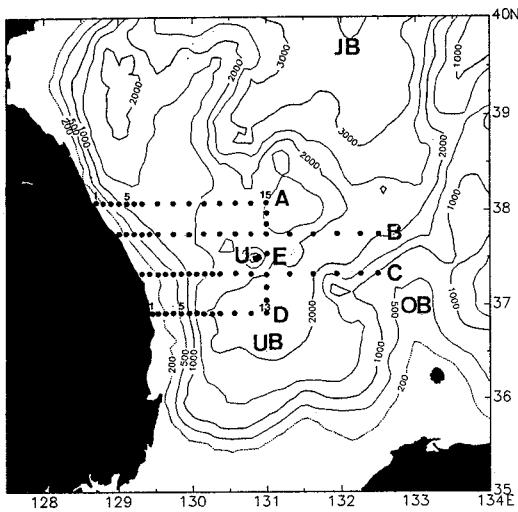
Fig. 1. Observational stations with bottom topography in meters. JB means Japan Basin; UB, Ulleung Basin; OB, Oki Bank; U, Ulleung island.

one meter intervals. Dynamic depths were calculated from water temperature, salinity and pressure at each station by using FORTRAN subroutine (UNESCO, 1991).

Current velocities were measured with ADCP (RD-SC0150) for ten minutes at each station during CTD observation, from surface to the depth of profiling range of 300 m, with bin length of 8 m and averaged to yield one vertical profile. Currents were measured by means of bottom tracking mode which took the bottom as a reference in the area where the sea bed was shallower than 350 m. In the area where bottom was deeper than 350 m, ADCP was operated by layer mode, which assumed a 'layer of no motion' as the depth from 274 m to 290 m.

Defant's method for the determination of the layer of no motion is searching the layer of relatively great thickness and considerably small vertical gradient from the analysis of differences in the dynamic depths of isobaric surface between two neighboring stations (Fomin, 1964). Variations of density structure in lower layer are weaker than those in upper layer in the East Sea. It was difficult to determine the layer of no motion because vertical profiles of differences in the dynamic depths of isobaric surface between two stations changed little below 100 m depth in shallow region and below 500 m depth in
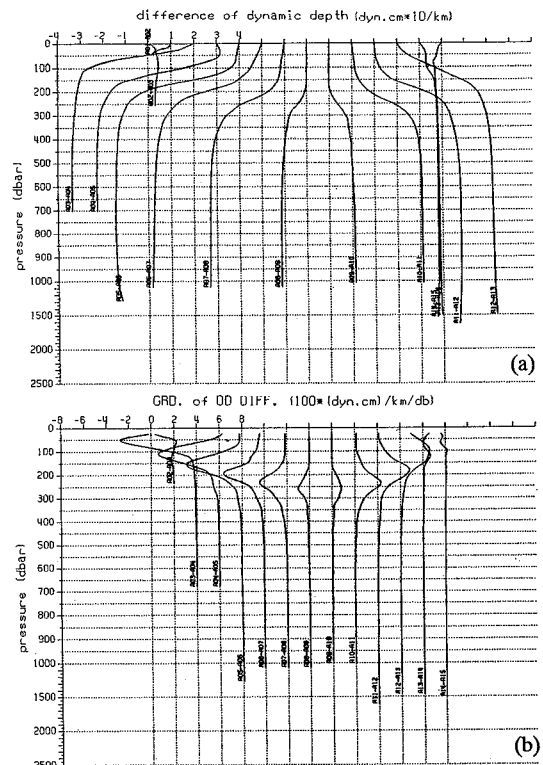

Fig. 2. (a) Vertical profiles of the differences in dynamic depth of isobaric surfaces between pairs of stations along the line A (Fig. 1) in March 1992. The names of station pairs are shown on left side of the end of the profiles. The differences of dynamic depth (dyn.cm $\times$ 10) were divided by distances (km) between pairs of stations. The origin of abscissa was shifted rightward with one unit for each curve. (b) Vertical gradients of the differences in dynamic depth (100 $\times$ (dyn.cm)/km/ db) depicted in Fig. 2 (a).

deep region (Fig. 2 (a)). Vertical gradients of the differences were calculated to easily determine the layer of no motion, which approached zero below 500~700 db (decibar) (Fig. 2 (b)). From this it was also difficult to select the layer of no motion in the vertical gradient profiles because the gradients are almost constant to zero below 500~700 db. Thus, any depth below 500~700 db can be considered as the layer of no motion, and consequently it has a minimal effect on the upper layer current distribution.

A closed box was made by the hydrographic lines A, E, D and the Korean coast (Fig. 1). Total volume transport was defined by the sum of input or output
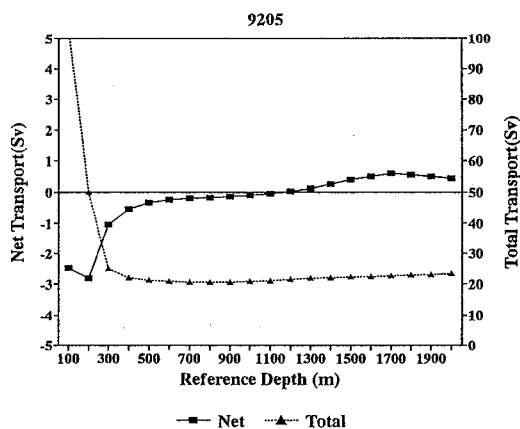
9205

Fig. 3. Volume transport as a function of reference level for the geostrophic calculation (May 1992). Solid line with filled square and broken line with filled triangle represent net transport and total transport respectively.

Fig. 4. Graphical illustration of dynamic depth extrapolation.

transports for the closed box, and net volume transport by the difference between input and output. If there is no sink, source, up- and down-welling in the closed box, the net geostrophic volume transport must be zero by the continuity. Thus, in this study, geostrophic currents were calculated by changing the level of no motion from 100 db to 2000 db by 100 db intervals, and then total and net transports were estimated. Finally the reference levels were determined by the depths where the net volume transport was minimum (Fig. 3). This net transport minimum method is more useful to choose layer of no motion than Defant's method in the study area.

To draw dynamic topography in the coastal area where bottom depth is shallower than reference layer, the dynamic depth was extrapolated by vertical gradient of the dynamic depth of the nearest station. Fig. 4 shows an illustration of extrapolation of the dynamic depth. In this case, the dynamic depth between "b" and "c" at St1 was extrapolated by the vertical gradient between "b" and "c" at St2, and dynamic depth between "c" and "d" at St1 was by the vertical gradient at St3. In the case of St2, dynamic depth extrapolation was carried out only in the depth from "c" to "d" using the gradient of the dynamic depth of St3. When calculating the geostrophic currents at the stations shallower than reference depth, this extrapolation method selects the
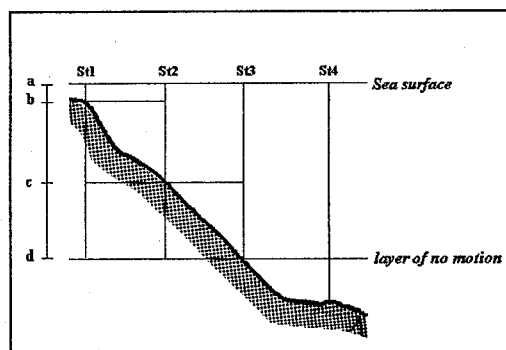
shallower bottom level as a reference depth because of the same dynamic depth between two stations from the layer of no motion to the shallower bottom level.

To compare the vertical profile with the same component of geostrophic current, the measured currents were averaged between station pairs, that is, a meridional component along the hydrographic lines A, B, C and D, and a zonal component along the hydrographic line E which connected station A15 and D13 (Fig. 1).

RESULTS AND DISCUSSIONS

The depth of the layer of no motion for every observation determined by the minimum net transport method is shown in Fig. 5. The reference depth varied in a wide range from 500 m in June 1992 and February 1993 to 1600 m in December 1992. This implies that the oceanographic condition vary actively in the southwestern East Sea. It is further necessary to study on the reason of the variation of the reference depth, even though it is beyond the scope of this study. Range of net volume transport calculated by the determined reference depth was $\pm 0.2 \times 10^6$ m^{3}s^{-1} and the ratio of input to output transports varied between -1$\pm$0.02 (Fig. 6). Thus, the layer of no motion was determined at the depth which the input (or output) transport was consistent with output (or input) transport of more than 98%.

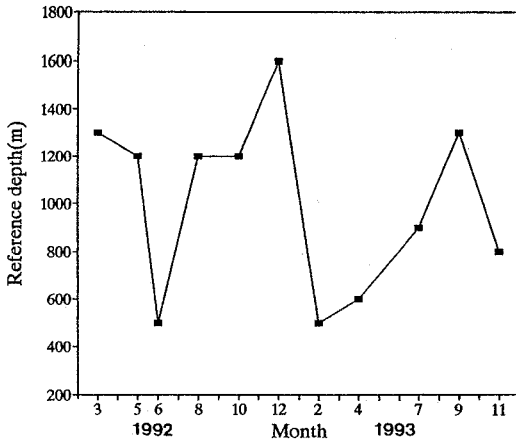Fig. 7 shows an example of dynamic topography and current vectors measured by ADCP in March

Fig. 5. Time variation of reference depth determined by continuity of volume transport in the box (closed by line A, E, D and Korean coast).
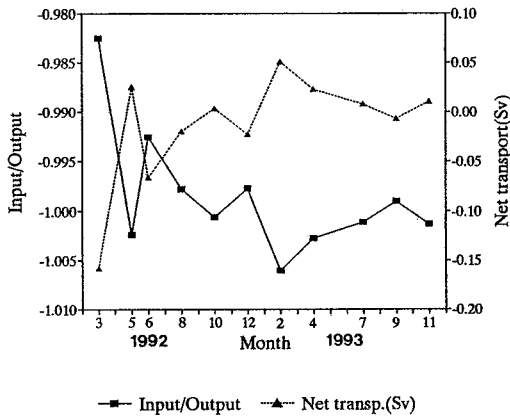

—■— Input/Output   —▲— Net transp.(Sv)

Fig. 6. Time variation of ratio of input/output transport and net transport in the box area. Solid line with filled square is for ratio of input/output and broken line with filled triangle for net transport.

Fig. 7. Dynamic topography (in J·kg⁻¹) of 10 m depth relative to 1300 m with current vectors measured by ADCP in March 1992. Vector scale is depicted at lower right corner.

1992. Dynamic topography contours clearly coincided with clockwise current of warm eddy reported by Shin *et. al.* (1995). The vertical profiles of geostrophic currents are very similar to those of the measured currents along line A in March 1992 even though there are some discrepancies in magnitude (Fig. 8).

The average of all the measured current speed from 10 m to 194 m depth was 11.6 cm s⁻¹ with standard deviation of 13.1 cm s⁻¹. Both mean and standard deviation were maximum at 10 m depth (mean; 18.5 cm s⁻¹, standard deviation; 16.3 cm s⁻¹). They de-
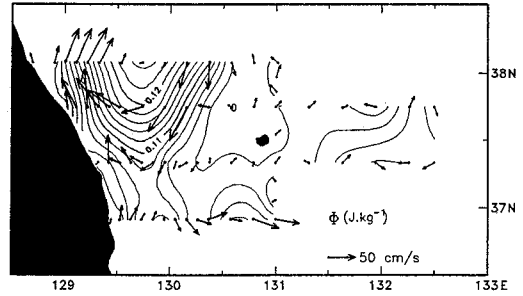
creased with increases in depth, and were minimal at 194 m (mean; 4.4 cm s⁻¹, standard deviation; 5.8 cm s⁻¹) (Fig. 9). To compare the geostrophic currents statistically with the measured currents, current data were selected in the upper layer from 10 m to 194 m depth because the measured current was as small as error (a few cm s⁻¹) at depths deeper than 200 m.

Correlation coefficients (r) between the measured currents and the geostrophic currents were higher than 0.80 except in February, September 1993, and in October 1992 when the lowest value 0.56 was shown (Fig. 10). The highest correlation coefficient occurred in March 1992 when warm eddy existed to the northwest of the Ulleung Island. Correlation coefficient of all the data was relatively high, valued at 0.83, which suggests good correlation between the measured and the geostrophic currents.

To analyze linear relationships, the measured currents were assumed by an independent variable (X) and the geostrophic currents by a dependent variable (Y). All of the 1st order coefficients (slopes) are within 1.00 ± 0.12 except in October 1992 and in February 1993 (Table 1). The slopes suggest nearly direct proportionality. Statistical significance can be tested by t-ratio and degrees of freedom (number of data - 2) at 95% confidence intervals about slope and constant (Y-intercept). All of the slopes are statistically significant. On the other hand, some Y-intercepts are statistically insignificant (March, August and December 1992, April 1993). However, physical reasons are weak because most of the Y-intercepts are smaller than ± 1.7 cm s⁻¹ which is very
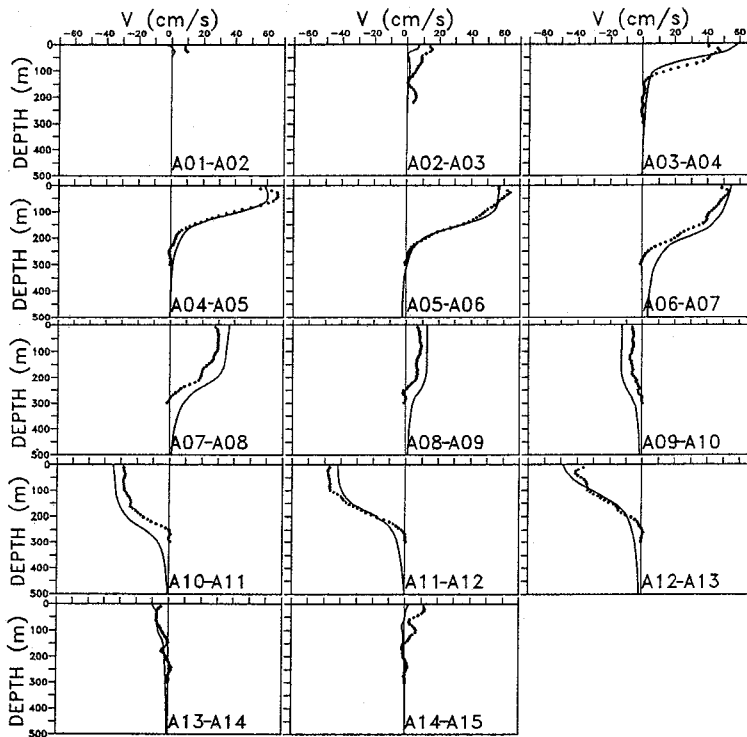
Fig. 8. Vertical profiles of geostrophic current (solid line) and averaged measured current (dots) between pairs of stations along line A in March 1992.
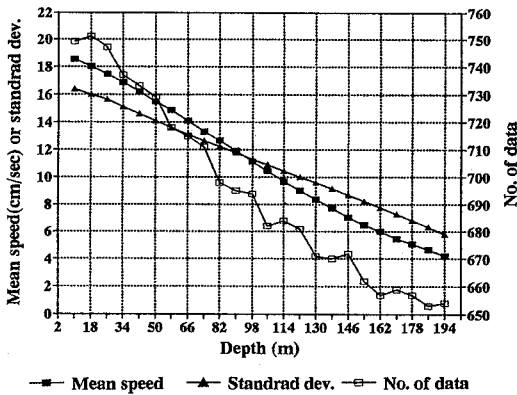

Fig. 9. Mean speed (cm s^{-1}), standard deviation and number of data with 8 m depth interval. Filled square, filled triangle and empty square indicate mean speed, standard deviation and number of data respectively.
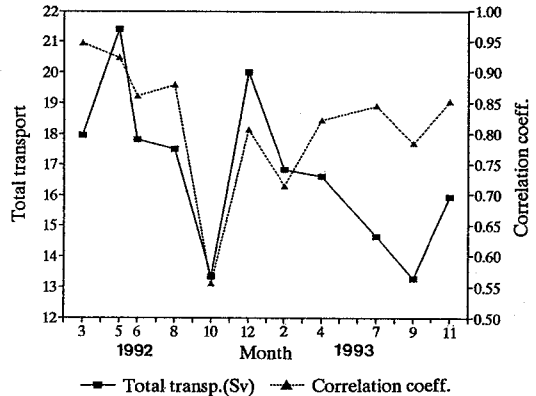

Fig. 10. Total transports (Sv; 10^6 m^{3}s^{-1}) in the closed area and correlation coefficients between geostrophic currents and measured currents. Solid line with filled square means total transport, broken line with filled triangle; correlation coefficient.

close to the error of current measurements except in October 1992.

The result of regression analysis of all the data showed that the slope is 0.91 and the Y-intercept is

0.95 cm s^{-1}. This fitted line (regression equation) explains 69.2% of the variation in the dependent variable Y (Table 1, Fig. 11 (a)). In the residual plot

Table 1. Results of linear regression analysis of geostrophic currents compared with currents by ADCP for 11 surveys.

| Observation time	No. of data	r^2	Constant	t ratio of const.	1st coef.	t ratio of 1st coef.
March, 1992	1547	0.897	-0.075	-0.446	1.020	115.671
May, 1992	1531	0.852	1.578	8.442	0.915	93.816
June, 1992	1536	0.741	1.744	7.357	0.944	66.347
August, 1992	1421	0.773	0.046	0.205	1.115	69.411
October, 1992	1535	0.308	3.511	11.971	0.592	26.098
December, 1992	1536	0.651	0.306	0.977	0.930	53.470
February, 1993	1538	0.510	1.502	5.687	0.695	39.969
April, 1993	1539	0.676	0.094	0.404	0.927	56.650
July, 1993	1540	0.714	1.470	8.271	0.981	61.611
September, 1993	1511	0.615	0.585	3.060	0.955	49.069
November, 1993	1535	0.726	-1.043	-4.868	0.926	63.611
Total	16769	0.692	0.947	13.188	0.911	193.838
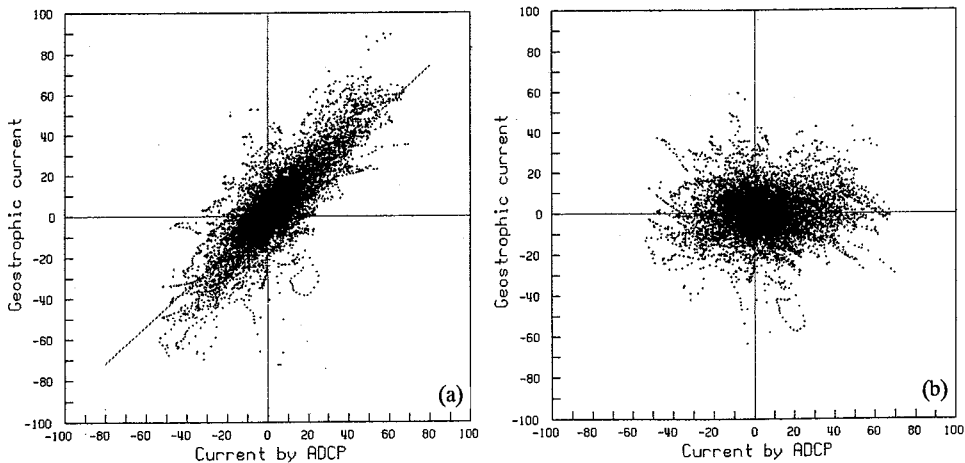
Fig. 11. (a) Relation of geostrophic currents (cm s^{-1}) and measured currents (cm s^{-1}). A dashed line indicates a regression line (geostrophic current = 0.95 + 0.91 × measured current). (b) Residuals result from the regression analysis.

(Fig. 11 (b)), the distribution of the residuals is centered around 0 and does not show any extreme tilting to one side or the other. These patterns are already accounted for by the regression line.

From studying the relation between the total transports in the closed box and the correlation coefficients (Fig. 10), the similar variation pattern can be seen. Fig. 12 demonstrates the trend clearly. Correlation coefficient between the total transport and the coefficient was 0.60. This correlation was statistically significant because the correlation is larger than critical values (0.5214) at the 10% testing level for a sample size 11 (Siegel, 1988). There is also a linear relationship between the total transport and the coefficient. This suggests that the stronger current implies the larger portion of geos-

trophic current and the better geostrophic balance in the study area. According to Pond and Pickard (1983), however, this relationship may have it's limitations, for example, the non-linear and frictional effects are comparable with Coriolis effect when current speed is larger than 100 cm s^{-1}.

To find out how much of the currents measured by ADCP are of the geostrophic component, percentages of geostrophic currents to measured currents were calculated from the individual data and classified the measured currents speed into intervals of 5 cm s^{-1} (Fig. 13). The mean for all the data was 68.7%, which can be interpreted that 68.7% of measured current speed was geostrophic. In low speed (v<5 cm s^{-1}) current, despite the amount of data (7300), mean percentage (59.6%) was not high and
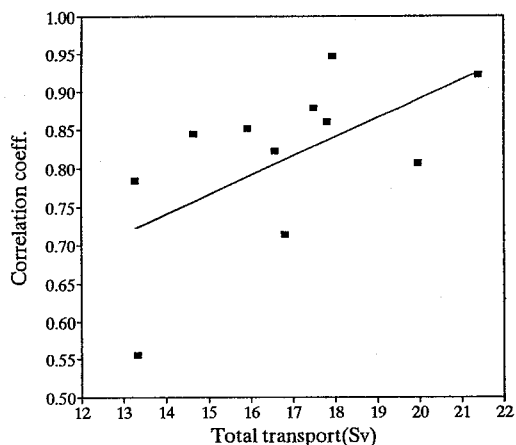
Fig. 12. Relationship of the correlation coefficient and the total transport. Solid line indicates regression line (correlation coefficient = 0.391 + 0.025 × total transport).

Fig. 13. Mean percentage (%), standard deviation and number of data for 5 cm s⁻¹ intervals. Percentage is the ratio of geostrophic current to the measured current. Filled square, filled triangle and empty square indicate mean percentage, standard deviation and number of data respectively.

standard deviation was very high. This is caused by low speed, that is, a small change of geostrophic current speed results in a large variation of ratio. The percentage increased with speed until 20 cm s⁻¹. From 20 cm s⁻¹ to 65 cm s⁻¹, average of the mean percentages was 78.2% which was larger than the mean for all the data. In the study area, tidal currents are very weak and bottom depth is relatively deep. Thus the current was little influenced by tides and bottom, then geostrophic balance may be accomplished. At high speed (65 cm s⁻¹<v), however, mean percentages decreased abruptly and the number of data was small, and confidence level was low.

There were some gradients of the difference of dynamic depth between pairs of stations approaching the center of the warm eddy where thermocline was deepened to 300 m depth at the station from A07 to A11 (Fig. 2(b)). The maximum range of the ADCP corresponds to the depth where the signal strength drops to the levels comparable to the noise level. Beyond this range the ADCP cannot accurately calculate Doppler shifts (RD instruments, 1989). Because of this limited profiling range, one cannot but operate ADCP by layer or ship tracking mode in deep sea. As mentioned before, ADCP was operated by the layer mode assuming layer of no motion about 300 m depth in the deeper area. Thus the observational error of current velocities occurred and the geostrophic cur-
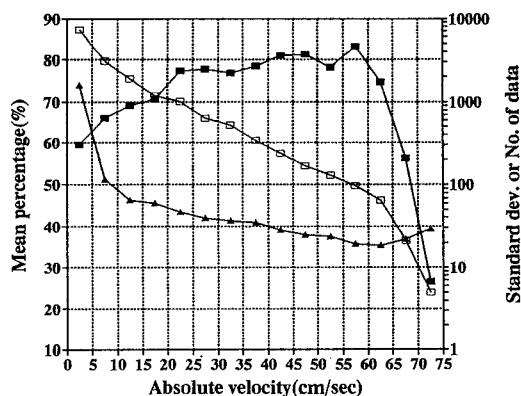
rents couldn't be compared with the current measured by ADCP beyond the maximum range. Also in this case, while most baroclinic (geostrophic) components were included in the measured currents, barotropic components were excluded.

Therefore, in order to get accurate current speed by extracting the ship speed precisely, it is necessary to operate ADCP with ship tracking mode using a precision navigation system such as the DGPS (Differential Global Positioning System). The calculation method of the geostrophic current will improve, for example, by choosing a level of no motion along isopycnal surface or inverse method. Also, there is need for a longitudinal study to get averaged phenomena.

CONCLUSION

In the southwestern East Sea, the geostrophic currents calculated from CTD data and the directly measured current by ADCP were statistically compared for the upper layer from 10 m to 194 m depth. To calculate geostrophic currents, the depth, where the net volume transport was minimum in the box closed by hydrographic lines and the Korean coast, was determined as the reference level. The ratios of input to output transports of the box varied between ±0.02.

Most of the correlation coefficients between the geostrophic current and the measured current were higher than 0.8. In the simple regression analysis for all the data, assuming the geostrophic current as a dependent variable, and the measured current as an independent variable, the slope was 0.91 and the Y-intercept was 0.95.

As the total transports increased, the correlation coefficients became larger. This suggests that the stronger the currents are, the better the geostrophic balance is. On the average, 68.7% of the measured current speed was geostrophic. In the speed range of $20\sim65$ cm s^{-1}, the mean percentage of 78.2% was higher than total mean, which was due to minimal effects of tides and bottom in the study area.

ACKNOWLEDGEMENTS

REFERENCES

Byun, S.-K. and Y.H. Seung, 1984. Description of current structure and coastal upwelling in the south-west Japan Sea-summer 1981 and spring 1982. In: Ocean hydrodynamics of the Japan and East China Seas, edited by T. Ichiye, Elsevier Science Publishers, Amsterdam, 83-93.

Fomin, L.M., 1964. The dynamic method in oceanography. Elsevier Publishing Company, Amsterdam, 212 pp.

Kaneko, A., S.-K. Byun, S.-D. Chang and M. Takahashi, 1991. An observation of sectional velocity structures and transport of the Tsushima current across the Korea Strait. Oceanography of Asian marginal seas, edited by K. Takano, Elsevier Science Publishers, Amsterdam, 179-195.

Lee, J.C. and C. Whang, 1981. On the seasonal variations of surface current in the eastern sea of Korea (August 1979-April 1980). *J. Oceanol. Soc. Korea*, **16(1)**: 1-11.

Lee, K.-B., 1978. Study on the coastal cold water near Ulsan. *J. Oceanol. Soc. Korea*, **13(2)**: 5-10.

Lie, H.-J. and S.-K. Byun, 1985. Summertime southward current along the east coast of Korea. *J. Oceanol. Soc. Korea*, **20(2)**: 22-27.

Lie, H.-J., S.-K. Byun, I. Bang and C.-H. Cho, 1995. Physical structure of eddies in the southwestern East Sea. *J. Korean Soc. Oceanogr.*, **30**: 170-183.

Ohwada, M. and K. Tanioka, 1972. Cruise report on the simultaneous observation of the Japan Sea in October 1969. *Oceanogr. Magazine*, **23(2)**: 47-58.

Pond, S. and G.L. Pickard, 1983. Introductory dynamical oceanography. 2nd ed. Pergamon press, Oxford, 329 pp.

RD instruments, 1989. Acoustic Doppler current profilers principles of operation: a practical primer, San Diego, California, 36 pp.

Seung, Y.H., 1974. A dynamic consideration on the temperature distribution in the east coast of Korea in August (in Korean). *J. Oceanol. Soc. Korea*, **9(1-2)**: 52-58.

Shin, H.-R., S.-K. Byun, C. Kim, S. Hwang and C.-W. Shin, 1995. The Characteristics of structure of warm eddy observed to the northwest of Ullungdo in 1992 (in Korean). *J. Korean Soc. Oceanogr.*, **30**, 39-56.

Siegel, A. F., 1988. Statistics and data analysis an introduction. John Wiley & Sons, New York, 523 pp.

UNESCO, 1991. Processing of oceanographic station data. 138 pp.